EFFECT OF HYDROTHERMAL CARBONIZATION TEMPERATURE ON FUEL PROPERTIES AND COMBUSTION BEHAVIOR OF HIGH-ASH CORN AND RICE STRAW HYDROCHAR

by

Zifeng SUI[a], Jie WU[a], Jiawei WANG[b], Yutong CAO[a], Qihao WANG[a], and Weipeng CHEN[a*]

[a] School of Energy and Environment,
Inner Mongolia University of Science and Technology, Baotou, China
[b] Key Laboratory of Condition Monitoring and Control for Power Plant Equipment,
Ministry of Education, North China Electric Power University, Beijing, China

Original scientific paper
https://doi.org/10.2298/TSCI220813186S

Hydrothermal carbonization has been proven to improve the fuel properties of low-ash straw biomass. To explore the effect of hydrothermal carbonization on high-ash straw biomass, the fuel properties and combustion behavior of hydrochar prepared by high-ash rice straw and corn straw at different temperature were studied. The results showed that increased reaction temperature could improve the C content, fixed carbon, heating value, and fuel ratios (FC/VM) in high-ash straw hydrochars, which is similar to the change trend of low-ash biomass. The hydrochar prepared at 260 °C has similar H/C and O/C atomic ratios and FC/VM to lignite. In addition, the highest energetic recovery efficiency is obtained at 200 °C. While at 180 °C, the comprehensive combustion characteristic index of the hydrochar is the best, which is $5.04 \cdot 10^{-11}$ *[*$min^{-2}K^{-3}$*] and* $6.42 \cdot 10^{-11}$ *[*$min^{-2}K^{-3}$*]. In addition, the C content in the hydrochars at 180 °C was lower than the raw material, and the ash content increases with the reaction temperature, which is quite different from the low-ash biomass. In conclusion, the hydrothermal carbonization could improve the fuel quality of high-ash straw, while its ash content remains at a high level.*

Key words: *high ash straw biomass, hydrothermal carbonization, combustion characteristics, reaction temperature*

Introduction

As an agricultural country, China is rich in crop straw biomass resources, which are an important part of agricultural waste [1]. In 2018, China's crop straw output was about 865 millionns, including rice, wheat, corn, beans and potato straw [2]. As a kind of easily accessible renewable resources, they have great potential for energy utilization, which is equivalent to about $2.54 \cdot 10^{13}$ KJ [3]. It could provide a way for realizing China's carbon emission peak and carbon neutrality [4].

How to use crop straw biomass for energy utilization have attracted the attention of many scholars. At present, various methods for straw biomass energy utilization have been proposed and studied, including direct combustion or combined combustion for power generation, and indirect use, such as hydrothermal carbonization (HTC), pyrolysis, liquefaction

* Corresponding author, e-mail: chenweipeng225@163.com

and gasification. When directly used as a fuel, compared to traditional fossil fuels, biomass, especially crop straw, has many disadvantages like low energy density, high ash content and high moisture content. In addition, crop straw has a low bulk density, which will result in an increment in storage and transportation cost [5]. Moreover, high alkali metal content, alkaline earth metal content, and silicon content in crop straw biomass would contribute to slagging and fouling of heat transfer surfaces, reducing overall thermal efficiency when it was directly burned [6]. Thus, more attention was paid to the study on the biomass indirect use method development and optimization, to improve its heating value and density, and decrease its ash content, moisture and so on.

As an emerging indirect use method, HTC technology, which is performed at mild reaction temperatures (180-260 °C) and pressure (autogenous pressure, 2-6 MPa) with water as the reaction medium, has been researched in many studies on the energy utilization of some lignocellulosic biomass, especially for low-ash crop straw [7, 8]. The HTC treatment could convert low-ash straw biomass into homogeneous, low-moisture and high-density solid fuel, with the ignition temperature and burnout temperature of hydrochar shifting to a higher temperature compared to the feedstock, and the chemical and combustion properties of the hydrochar are improved [9-11]. In some studies, it is found that the energy density of hydrochar, the solid product of HTC, is close to peat and lignite, and it could be used as clean fuel for direct combustion [12]. During HTC, biomass underwent hydrolysis, dehydration, decarboxylation, aromatization and recondensation reactions, in which dehydration and decarboxylation can reduce the H/C and O/C ratios of biomass, thus forming high value-added products, such as solid fuel and electrode materials [13-16]. In addition, it is proved that the HTC process is mainly affected by reaction temperature [4].

However, there are few studies on high-ash biomass, and the conclusions of relative research are not uniform at present. Khoo *et al*. [17] conducted HTC research on high-ash microalgal biomass and found that the hydrochar had a higher heating value (HHV), which was proximately two-times higher than that of raw biomass. However, Xu *et al*. [18] found that after HTC of high ash rice husks, the ash content of the hydrochars increases greatly, but the heating value increases less. Therefore, it is necessary to continue related research.

In order to develop the different reaction conditions that can be applied to convert high-ash crop straw to clean fuel, the effects of reaction temperature on the physicochemical properties and combustion behavior of hydrochar produced by high-ash crop straw were tested and analyzed. The properties and combustion characteristics of hydrochar were studied by proximate analysis, ultimate analysis, Fourier transform infrared spectroscopy analysis, and thermogravimetric analysis. The research results of this study could provide an important theoretical basis for the design and optimization of the high ash crop straw HTC technology in energy applications.

Materials and methods

Experimental materials and hydrothermal carbonization treatment

Rice straw (RS) and corn straw (CS) with a particle size of 200 mesh (less than 75 μm), produced from Lianyungang City, Jiangsu province, China, would be used in the experiment. Before the experiment, RS and CS straw powders were dried at 105 °C for 24 hours.

In order to prepare hydrochar samples, the HTC experiments of RS and CS were carried out by using an autoclave (FCF-1L, Shanghai Qiuzuo Scientific Instrument Co., Ltd., China). Firstly, 50 g straw powder and 500 ml deionized water were mixed and poured into the

autoclave. Seal the autoclave and purge it with high-purity nitrogen to discharge the air. The reactor is heated to the preset reaction temperature. Then, the reaction temperature was kept for 60 minutes. The stirring speed is 500 rpm during the HTC process. After the reaction was completed, the autoclave was fast-cooled to the ambient temperature by water (below 50 °C). The solid matter in the mixture was filtered out and dried at 105 °C for 24 hours to obtain a hydrochar sample for subsequent analysis. To analyze the effects of reaction temperature on hydrochar, the experiments of control variables were carried out under five reaction temperatures (180 °C, 200 °C, 220 °C, 240 °C, and 260 °C), respectively.

Analytical methods

– Ultimate analysis, proximate analysis and HHV

The ultimate analysis and proximate analysis of hydrochar were tested by ultimate analyzer (EA3000, EURO, USA) and automatic proximate analyzer (TGA701S4C, LEGO, USA). The content of oxygen (O) and fixed carbon (FC) is obtained by subtraction method. The high heating value (HHV, KJ/kg) is calculated by eqs. (1) [19]:

$$HHV = 3.55C^2 - 232C - 2230H + 51.2C \times H + 131N + 20600 \tag{1}$$

where C, H, and N are the carbon, hydrogen, and nitrogen contents of RS and CS biomass or hydrochar, respectively, expressed as a percentage of dry basis.

– Fuel analysis

Hydrochar yield M_Y [%], energy densification E_D, energetic recovery efficiency E_Y [%] was determined:

$$M_Y = \frac{m_{\text{hydrochar}}}{m_{\text{raw}}} \times 100 \ [\%] \tag{2}$$

$$E_D = \frac{HHV_{\text{hydrochar}}}{HHV_{\text{raw}}} \tag{3}$$

$$E_Y = M_Y \times E_D \ [\%] \tag{4}$$

where $m_{\text{hydrochar}}$ is mass of hydrochar, m_{raw} – mass of raw sample, $\text{HHV}_{\text{hydrochar}}$ – high heating value of hydrochar, and HHV_{raw} – high heating value of raw sample.

– Fourier transform infrared spectroscopy (FTIR)

The FTIR was an effective method to investigate the functional group of solid sample. The functional group of hydrochar was investigated by a FTIR spectrometer. The sample was scanned in 4000-400 cm^{-1} region with a resolution of 4 cm^{-1}, and 4 scan.

– Thermo-gravimetric analysis

The comprehensive thermal analyzer (HCT-4, Beijing Hengjiu Experimental Equipment Co., Ltd., China) is employed for TGA testing. The sample mass is 5 ± 0.5 mg, the temperature range is from ambient temperature to 800 °C, the heating rate is 10 °C per minute, and the air-flow rate is 100 ml per minute.

Based on the TG-DTG curve, the tangent method is used to determine the combustion parameters of straw biomass, such as ignition temperature, T_i, burnout temperature, T_b, maximum weight loss rate, DTG_{max}, and temperature, T_{max}, and corresponding to DTG_{max} [20].

– Determination of combustion characteristic index

The comprehensive combustibility index, S_N, [21] and decrement of flammability index, S_W, [22] are effective indicators for evaluating the combustion characteristics of samples, with the specific meanings as follows.

Comprehensive combustibility index S_N [10^{-11}min^{-2}K^{-3}] represents the comprehensive combustion characteristics. The larger the S_N means the better the comprehensive combustion characteristics of the fuel. The S_N was calculated using:

$$S_N = \frac{DTG_{\max} \times DTG_{\text{mean}}}{T_i^2 \times T_b} \tag{5}$$

where DTG_{mean} [% per minute] is the average weight loss rate, which is the average weight loss rate from the beginning to the end of the weight loss of the sample:

$$DTG_{\text{mean}} = \beta \frac{\alpha_i - \alpha_b}{T_i - T_b}$$

where β is the heating rate, taking 10 °C per minute, α_i [%] – the percentage of remaining samples corresponding to the ignition temperature point, and α_b [%] – the percentage of remaining samples corresponding to the burnout temperature point.

Flammability index S_w [10^{-7}min^{-1}K^{-2}] is the parameter of combustion reaction capacity after the fuel reaches T_i in the early stage of reaction. The larger the S_w means the better flammability. The S_w was calculated using:

$$S_w = \frac{DTG_{\max}}{T_i^2} \tag{6}$$

– Combustion kinetics analysis

The activation energy, E, and pre-exponential factor, A, of biomass hydrochar combustion was determined by Coats-Redfem method, which is widely used in the researches of combustion kinetic parameters [4, 10]. This method is a mathematical model for calculating the TG parameters of constant heating rate. The calculation model:

$$\frac{1-(1-\alpha)^{1-n}}{1-n} = \frac{ART^2}{\beta E}\left[1-\frac{2\text{R}T}{E}\right]\text{e}^{-E/\text{RT}} \tag{7}$$

where A [min^{-1}] is the pre-exponential factor, α – the degree of conversion, which can be obtained from the TG tests, n is the order of reaction, R [8.314 Jmol^{-1}K^{-1}] – the gas constant, T [K] – the temperature, and β [Kmin^{-1}] – the heating rate.

Solid fuel combustion is a very complex process and can be thought of as a simple reaction sequence step: Hydrochar + $O_2 \rightarrow CO_2 + H_2O$. The entire combustion process is divided into two combustion stages where volatiles are released and the fixed carbon is burned. Each combustion stage is considered to be a single first-order chemical. Thus, the kinetic equations of these two-stages are fitted with the reaction order $n = 1$, and the Coats-Redfern method was used to calculate the kinetic parameters [23, 24]:

$$\ln\left[\frac{-\ln(1-\alpha)}{T^2}\right] = -\frac{E}{\text{R}}\frac{1}{T} + \ln\left[\frac{A\text{R}}{\beta E}\left(1-\frac{2\text{R}T}{E}\right)\right] \tag{8}$$

As term $2\text{R}T/E \ll 1$, $\ln[A\text{R}/\beta E(1 - 2\text{R}T/E)]$ could be regard as a constant. According to the equation of kinetic principle, when the reaction order $n = 1$, $\ln[-\ln(1 - \alpha)/T^2]$ can be fitted with $1/T$ to form a straight line [4]. Plotting the value on the left side of eq. (8) against the value of $1/T$ (the temperature was selected from the temperature range of volatile release combustion stage and fixed carbon combustion stage) and fitting a straight line to these data, the E from the slope was determined. Due to β and R are constant. The pre-exponential constant, A, can be calculated from the intercept. In addition, the correlation coefficient, R^2, in the calculation

process is all above 0.95, indicating that this order of reaction kinetics can be used to study the combustion kinetics of straw and hydrochars [4, 10, 25].

Results and discussion

Hydrochar yield, energy densification, energetic recovery efficiency

The effect of temperature on the M_Y, E_D, and E_Y was shown in tab. 1. It is shown that the M_Y decreases, the E_D slightly increases as the growth of reaction temperature. To be specific, the M_Y of RS and CS hydrochars decreased by 15.36%, 16.85%, respectively, when the temperature increased from 180-260 °C. It is mainly because hemicellulose (decomposed at 180 °C) and cellulose (decomposed at 220 °C) were decomposed into monomers and oligomers, and more matter could be decomposed with the temperature increase [21]. The E_D of RS and CS hydrochars slightly increased 0.11 and 0.18, respectively, from 180-260 °C. It could be attributed to the decomposition of cellulose and hemicellulose in the HTC process, while increases the relative content of lignin, and the higher content of lignin increases its energy densification [26]. The reaction temperature benefited in the upgradation of E_D. Based on the M_Y and E_D values, the E_Y of hydrochars was calculated and shows a trend of first increasing and then decreasing with the increase of reaction temperature. Thus, it is suggested that higher reaction temperature has negative effect on the E_Y of hydrochars.

Table 1. Effect of reaction temperature on M_Y, E_D, E_Y

Sample	M_Y [%]	E_D	E_Y [%]
RS180	65.56	0.98	64.39
RS200	65.01	1.02	66.62
RS220	62.30	1.04	64.82
RS240	55.97	1.07	59.68
RS260	50.20	1.09	54.90
CS180	61.74	1.00	61.74
CS200	60.94	1.06	64.39
CS220	57.76	1.07	61.90
CS240	52.31	1.10	57.69
CS260	44.89	1.18	53.12

Ultimate and proximate analysis

The ultimate and proximate analysis results (dry basis) at different reaction temperatures were listed in fig. 1, and S content was not shown in fig. 4 because it could not be detected in RS and hydrochars. During the HTC process, the C content was changed significantly compared with the raw materials. The C content in the hydrochar slightly decreased at 180 °C. When the temperature continues to increase, it generally shows an upward trend. Under the condition of 260 °C, the C content of RS and CS hydrochars increased to 43.03% and 51.13%, respectively. The law in the HTC of straw biomass is different from the consistent rising law in the study of Ma *et al.* [10] which could be due to ash content variations in the raw materials. As shown in fig. 1(b), the proximate analysis found that the FC content in the RS and CS hydrochars had the similar trend of change.

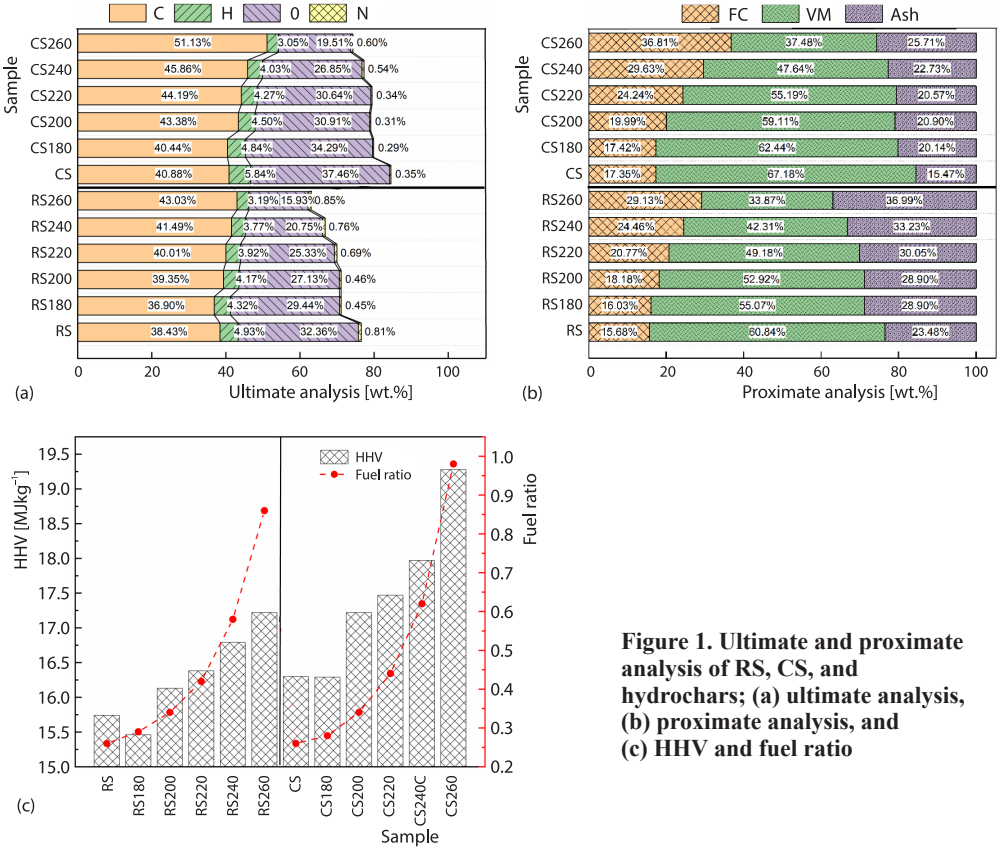

Figure 1. Ultimate and proximate analysis of RS, CS, and hydrochars; (a) ultimate analysis, (b) proximate analysis, and (c) HHV and fuel ratio

The high ash biomass has an ash content of 11.3-28.00% [17, 18]. The ash contents of the RS and CS feedstocks were 23.48% and 15.47%, respectively, as shown in fig. 1(b). The ash content of RS hydrochar and CS hydrochar increased sharply from 23.48-28.90% at 180 °C, and the ash content of CS hydrochar increased from 15.47-20.14 % at 180 °C, which makes the C content of hydrochar in dry basis appear to be slight reduced. If converted to dry ash-free base, the C content of hydrochars increases at 180 °C compared with raw material. As the reaction temperature continues to increase, it is found that the ash content of hydrochar presents a trend of slow increase. However, some other previous works argued that the change trend of ash content of low-ash straw biomass after HTC was different [9-11]. An increase of ash in the hydrochar is observed, due to excessive loss of volatile matter, retention of minerals and degradation of organic substances [27]. A similar trend was found in the HTC of eucalyptus bark waste, rice husk and grape residue [28].

In addition, the content of H and O at different HTC temperatures has changed significantly, which has the same trend as the HTC of low-ash biomass [29]. The content of H decreased from 4.93% in raw RS to 3.19% at 260 °C, and the content of O decreased from 32.36% in raw RS to 15.93% at 260 °C. In the process of CS HTC, when the reaction temperature was increased from 180-260 °C, the content of H decreased significantly, from 5.84-3.05%, and the content of O decreased from 37.46-19.51%. The removal of H and O contents were attributed to continuous strengthening dehydration and decarboxylation during the HTC process [30]. The hydrogen and oxygen components in biomass were cracked, decomposed and eventually

evolved out as gases such as H_2, CH_4, CO_2, and H_2O [4]. Besides, the hydrophobic of hydrochar improved gradually as the oxygen-containing functional groups (such as carboxyl carbonyl) decreased [31].

Table 2. The HHV and fuel ratio of hydrochar produced at different reaction temperature

Sample	RS	RS180	RS200	RS220	RS240	RS260	CS	CS180	CS200	CS220	CS240	CS260
HHV [MJkg^{-1}]	15.74	15.46	16.13	16.38	16.79	17.22	16.30	16.29	17.22	17.47	17.97	19.28
Fuel ratio	0.26	0.29	0.34	0.42	0.58	0.86	0.26	0.28	0.34	0.44	0.62	0.98

Meanwhile, heating value and the FC/VM can be used as an indicator to evaluate the feasibility of biomass to replace fossil fuels. The heating value of RS and CS are 15.74 MJ/kg and 16.30 MJ/kg, respectively, as shown in fig. 1(c) and tab. 2, which are lower than the 16.41 MJ/kg of rice straw studied by Zhang [32] and the 18.22 MJ/kg of corn stover studied by Wang *et al*. [11], which may be due to the high ash content in the original straw biomass, and the higher ash content may lead to the low heating value of the straw biomass. Compared with RS and CS, it could be observed that an obvious upgradation in HHV of hydrochar was achieved with increasing reaction temperature. The HHV of RS and CS increased to 17.22 MJ/kg and 19.28 MJ/kg at 260 °C, respectively, which was similar to the HHV of lignite (15-20 MJ/kg) [33]. This phenomenon could be explained as cellulose and hemicellulose in feedstocks decomposed gradually as HTC progressed, thus leaving products with higher lignin content [34]. Moreover, the fuel ratio of RS and CS increased from 0.26 and 0.26-0.86 and 0.98, respectively, with increasing HTC reaction temperature. The variation of fuel ratio is the same as the HTC of corncob with low ash content studied by Zhang *et al*. [35]. The fuel ratio was related to the change of FC and VM contents during the HTC process. Significantly, the fuel ratio changes dramatically from 240-260 °C. This may be due to the intense dehydration of RS and CS under this reaction condition. In summary, higher reaction temperatures promote dehydration and decarboxylation in the HTC process, and increase HHV [36]. The HTC could be used as a new way to improve the crop straw HHV, and then improve the combustion quality of the crop straw. This is consistent with the phenomenon of the Van Krevelen diagram, fig. 2, and with the results of fig. 1.

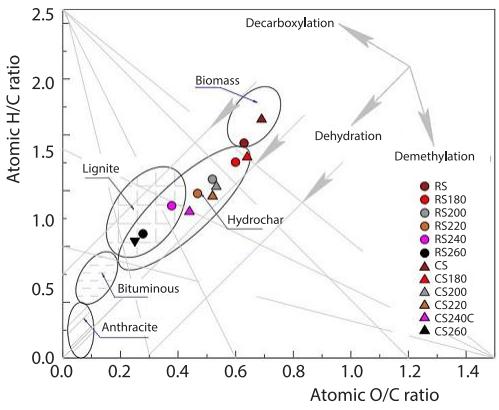

Figure 2. Van Krevelen diagram for RS, CS, and hydrochars

In order to deeply analyze the mechanism of HTC, relationships among H/C and O/C ratios of crop straw and hydrochar samples were indicated in the Van Krevelen diagram, fig. 2. It can be seen that the evolution of the H/C and O/C ratios from crop straw to hydrochars followed the paths of dehydration reactions. In addition, H/C and O/C atomic ratios of hydrochar decreases gradually with the increase of reaction temperature, which is similar to the change of the atomic ratio during the HTC of low-ash rape straw by Cheng *et al.* [9]. It was found that the H/C and O/C atomic ratios of lignite are usually 0.8-1.3 and 0.2-0.38, respectively [37]. At a high reaction temperature (260 °C), the position of hydrochar atomic ratios was closer to lignite regions. This might be because the dehydration of biomass straw was enhanced with the

increase of reaction temperature. Therefore, high reaction temperatures can improve the degree of coalification in hydrochar. A noteworthy finding was that the H/C and O/C atomic ratios had a large mutation at 260 °C. This represented that the hydrolysis of cellulose and hemicellulose in RS and CS was most severe at this reaction temperature. In fact, the reduced O/C atomic ratios were attributed to decarboxylation and dehydration, and this decreased H/C atomic ratio is mainly due to dehydration and aromatization in the HTC process, which help to avoid the energy loss of flue gas and steam in the combustion process of hydrochar as a clean energy source [38].

In conclusion, based on the HTC, compared with raw materials, the product of hydrochar at 260 °C has higher C content, lower H and O content, higher HHV, fuel ratio and energy densification, indicating that HTC treatment can improve the fuel quality of the crop straw. However, the ash content of the hydrochars also remains high.

Functional group analyses of RS, CS, and hydrochars

The FTIR analysis of RS, CS, and hydrochar can reveal the evolution of functional groups in samples at different reaction temperatures. The FTIR spectra of RS, CS, and hydrochar samples are shown in fig. 3. The absorption bands at approximately 3400 cm^{-1} were attributed to stretching vibrations of -OH, which became less intense after the increase of reaction temperature, indicating the enhanced dehydration reaction [5]. The absorbance peaks between 2924 cm^{-1} and 2918 cm^{-1} were associated with -C-H stretching vibration in methyl, methylene, and groups, and showed no prominent fluctuation [39, 40]. Peaks from 1770-1650 cm^{-1} were assigned to -C=O stretching vibration in carboxyl. The absorbance intensity was weakened with increasing reaction temperature, which also confirmed that the high reaction temperature promoted the decarboxylation reaction. Moreover, the decrease of -OH and -C=O implied that the HTC could efficiently improve the hydrophobicity of hydrochars [21]. The absorbance Peaks at 1733 cm^{-1} and 1247 cm^{-1} were denoted the -C=O and -C-O stretching vibration of esters, carboxylic acids or aldehydes from hemicellulose, respectively. The intensity of these absorbance peaks notably decreased following hydrothermal treatment and they nearly disappeared entirely for treatments above 180 °C, indicating that hemicellulose began to hydrolyze at 180 °C [10]. The increasing intensity of peaks at approximately 1605 cm^{-1}, which was assigned to -C=C vibrations of the aromatic ringsin lignin. With the increase of the reaction temperature in the HTC process, the appearance of a shoulder around 2918-2924 cm^{-1} and the absorbance peak at 802 cm^{-1} (-CH aromatic vibration) suggest an increase in aromatic character during carbonization [6]. The absorption bands between 1380 cm^{-1} and 1310 cm^{-1} and between 1214 cm^{-1} and 1030 cm^{-1} were mainly attributed to the vibration of methoxy group ($R\text{-}O\text{-}CH_3$) and ether group (C-O-C), respectively. Similarly, the vibration intensity was weakened with the increase of temperature, suggesting that high temperatures might accelerate the deoxygenation reaction of the crop straw during the HTC process [21]. The absorbance peak at 898 cm^{-1} represented for β-(1-4)-glycosidic bond (C-O-C). The vibration intensity experienced a downtrend around 200 °C, indicating that evidence of the onset of the cellulose-hydrolysis reaction [10]. It could be observed that hemicellulose and cellulose destruction and increasing aromatization with increasing HTC temperature. This was in conformity with the aforementioned results of ultimate analysis and proximate analysis. In summary, after HTC of straw biomass, cellulose and hemicellulose were hydrolyzed and decomposed. With the increase of the reaction temperature, the dehydration and decarboxylation of the hydrochars was intensified, the degree of aromatization was deepened, and the hydroxyl and carboxyl groups were reduced, which effectively improved its hydrophobicity.

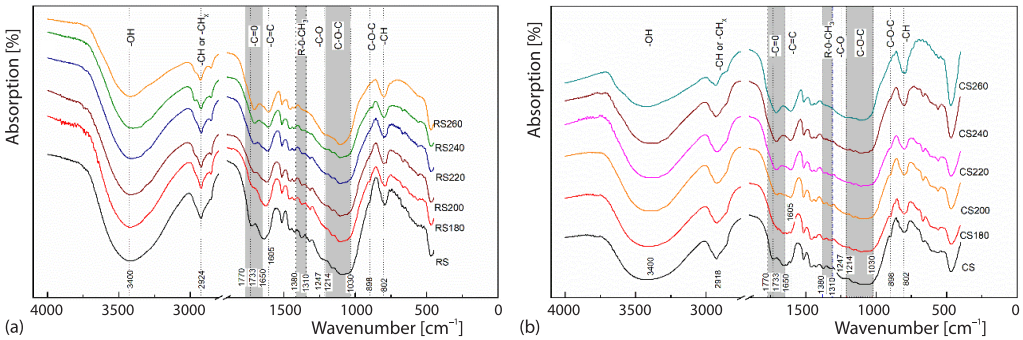

Figure 3. The FTIR spectra of RS, CS, and hydrochars; (a) RS and (b) CS

Combustion behavior

The TG and DTG of RS, CS, and hydrochars were shown in fig 4. For better evaluation of the combustion behavior, as indicated in figs. 4(b) and figs. 4(d), the main combustion processes of RS, CS and hydrochars could be divided into two-stages. The weight loss peak of Stage I between 210 °C and 370 °C, revealed that the low boiling point compounds in crop straw and hydrochars were volatilized, and hemicellulose, part of lignin and cellulose were pyrolyzed, during which a large number of volatiles were generated. The weight loss peak of Stage II from 370-550 °C was attributed to the combustion of fixed carbon, indicating that a small amount of volatiles and a large amount of carbon are generated from lignin pyrolysis, followed by combustion on the surface of carbon in this process [40]. At Stage I, the straw biomass after HTC with increasing temperature, the weight loss peak maintained a gradual downtrend, suggesting that the VM content had a decreasing trend, which was in accordance with proximate analysis. At the Stage II, the weight loss peak reduced when the reaction temperature is 180 °C, resulting from the chemical components contained in RS and CS decomposing to generate hydrochars that possessed complex structures via aromatization and repolymerization reactions. The hydrocars may have stable benzene ring structures and low reaction activity, which makes it more difficult for combustion at the Stage II. As the reaction temperature continues to increase, it is found that the weight loss peak of hydrochar presents a trend of increase. This phenomenon could be due to the decomposition of new complex chemical structures and the increase of fixed carbon at higher reaction temperatures [29]. During the HTC process, it could be observed that the weight loss peak at the Stage II moved to the higher temperature region gradually. This could be attributed to higher reaction temperatures increasing the content of fixed carbon in hydrochars.

The combustion characteristic parameters of RS, CS, and hydrocars are given in tab. 3. After RS and CS were treated by HTC, their T_i and T_b changed. Compared with RS and CS, the T_i of hydrochars has increased. The RS hydrochar produced at 180 °C and the CS hydrochar produced at 200 °C all showed the highest T_i. Increasing the T_i of hydrochars is more beneficial to prevent fire and reduce the risk of explosion [41]. The T_i is related to volatile material content, particle size, surface area and contact with oxygen [42]. At 260 °C, the T_b of RS and CS hydrochars became higher, which reached 500.05 °C and 577.51 °C, respectively. In fact, higher T_b may mean that the hydrochar combustion process takes longer to occur, which may ultimately release more energy and less residue after combustion [43].

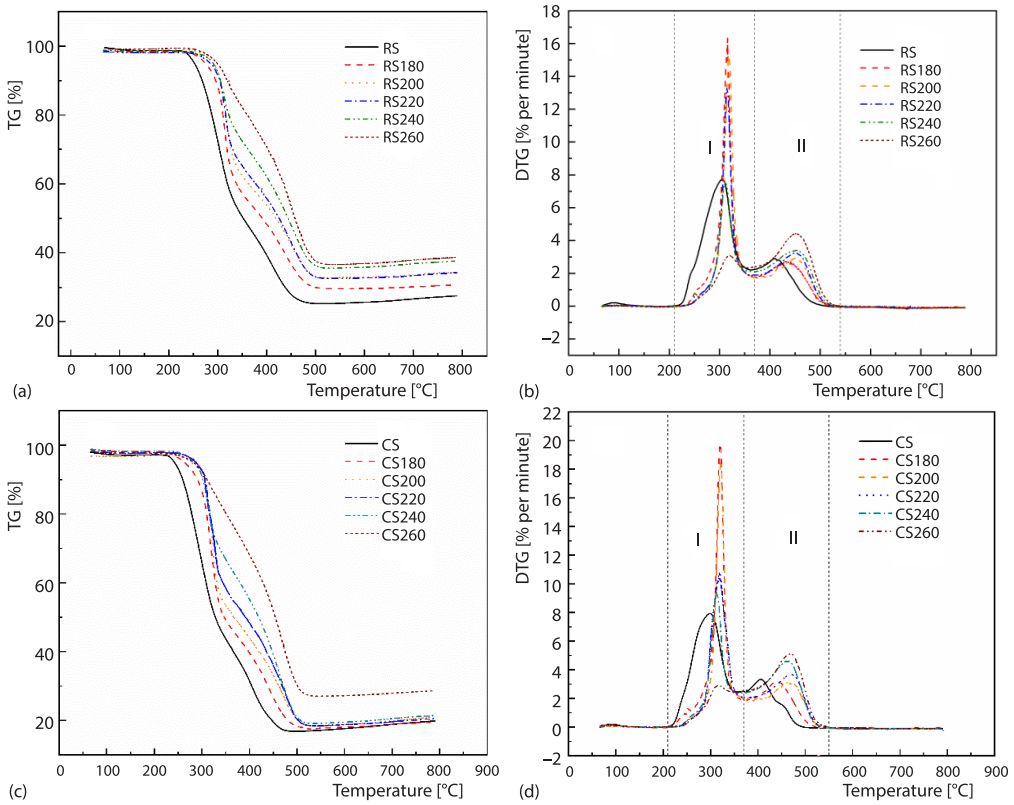

Figure 4. The TG and DTG profiles of straw hydrochars; (a) TG of RS hydrochar samples, (b) DTG of RS hydrochar samples, (c) TG of CS hydrochar samples, and (d) DTG of CS hydrochar samples

Table 3. The combustion characteristics parameters of RS, CS and hydrochars

Sample	T_i [°C]	T_b [°C]	DTG_{mean} [% per minute]	S_N [10^{-11}min^{-2}K^{-3}]	S_w [10^{-7}min^{-1}K^{-2}]
RS	260.00	368.00	4.34	1.88	2.78
RS180	297.50	348.40	6.23	5.04	5.03
RS200	295.73	368.16	4.76	3.51	4.73
RS220	296.74	363.32	4.83	3.46	4.56
RS240	292.44	386.36	3.16	1.14	2.38
RS260	289.14	500.05	2.78	0.39	1.07
CS	252.12	373.19	4.47	1.99	2.87
CS180	292.99	363.87	6.30	6.42	6.15
CS200	307.71	353.44	7.73	6.36	5.16
CS220	300.76	374.74	5.32	2.67	3.25
CS240	293.85	388.18	3.70	1.64	2.93
CS260	274.23	577.51	2.28	0.26	0.97

The comprehensive combustibility index S_N values of RS and CS hydrochars were $5.04 \cdot 10^{-11}$ [$min^{-2}K^{-3}$] and $6.42 \cdot 10^{-11}$ [$min^{-2}K^{-3}$] at 180 °C, respectively, which were superior to all other samples and showed better combustion performance. Similarly, some other previous works found that biomass with low ash content, such as deciduous trees, bushes, bamboo and wheat straw, *etc.* showed better S_N at low temperature stage (180-200 °C) during HTC, with similar results [4, 10, 29, 40]. With the increase of reaction temperature, the S_N value of RS and CS hydrochars decreased to $0.39 \cdot 10^{-11}$ [$min^{-2}K^{-3}$] and $0.26 \cdot 10^{-11}$ [$min^{-2}K^{-3}$] at 260 °C, respectively. It suggests that the increase of reaction temperature had a negative effect on the improvement of the S_N value of hydrochars. The reasons for the previous phenomenon are as follows. Firstly, in the temperature range of 180-260 °C, the content of VM declined sharply, due to VM could improve the flame burning, resulting from the S_N also had a significant decrease. Moreover, the specific surface area and porosity of hydrochar usually increase to 230 °C, further increase represents negative response. The larger specific surface area was more violently and easily hydrochar burned. These two factors may had a synergistic effect [4]. At 180 °C, hydrochar had high VM content and large specific surface area, which was the most intense in the combustion process. Therefore, the combustion performance of hydrochar showed the highest S_N and S_w at this temperature.

Kinetic analysis

The E and A parameters are the basis for understanding the combustion process. The E is used to estimate the energy barrier involved in the combustion reaction stage, while A represents the reaction collision frequency, taking into account reactant orientation and solid fuel contact surface [13]. The results of kinetic analysis were exhibited in tab. 4. The E of RS and hydrochars at the Stages I and II was, respectively in the range of 66.17-85.45 KJ/mol and 22.43-50.24 KJ/mol with respect to different HTC temperatures. While the combustion E of CS and hydrochars at Stages I and II was 43.01-89.72 KJ/mol and 19.83-45.31 KJ/mol, respectively. In the Stage I, the maximum $E_{\text{stage I}}$ of RS and CS hydrochar is at 200 °C, and the $E_{\text{stage I}}$ decreases as the reaction temperature continues to increase. It is attributed to the HTC

Table 4. Kinetic parameters for combustion of RS, CS, and hydrochars

Sample	Stage I				Stage II			
	Temperature range [°C]	E [KJmol^{-1}]	A [min^{-1}]	R^2	Temperature range [°C]	E [KJmol^{-1}]	A [min^{-1}]	R^2
RS	200-355	75.26	$2.15 \cdot 10^{07}$	0.972	370-440	40.15	$7.51 \cdot 10^{03}$	0.955
RS180	230-370	78.93	$2.80 \cdot 10^{07}$	0.968	380-440	28.88	$5.27 \cdot 10^{02}$	0.960
RS200	225-375	85.45	$8.20 \cdot 10^{07}$	0.954	380-450	22.43	$1.15 \cdot 10^{02}$	0.972
RS220	230-360	78.36	$1.99 \cdot 10^{07}$	0.952	370-450	27.20	$3.02 \cdot 10^{02}$	0.958
RS240	235-350	77.50	$1.41 \cdot 10^{07}$	0.954	370-460	36.25	$1.71 \cdot 10^{03}$	0.964
RS260	210-360	66.17	$6.69 \cdot 10^{05}$	0.963	370-470	50.24	$2.01 \cdot 10^{04}$	0.962
CS	200-350	62.62	$1.52 \cdot 10^{06}$	0.969	380-440	45.31	$2.23 \cdot 10^{04}$	0.977
CS180	210-365	66.77	$2.00 \cdot 10^{06}$	0.953	380-440	22.59	$1.35 \cdot 10^{02}$	0.958
CS200	255-360	89.72	$2.30 \cdot 10^{08}$	0.950	390-440	19.83	$6.34 \cdot 10^{01}$	0.959
CS220	250-370	87.68	$1.20 \cdot 10^{08}$	0.950	380-450	20.32	$6.09 \cdot 10^{01}$	0.942
CS240	225-365	69.25	$2.12 \cdot 10^{06}$	0.955	370-460	29.90	$4.06 \cdot 10^{02}$	0.961
CS260	225-350	43.01	$4.54 \cdot 10^{03}$	0.957	370-470	40.33	$2.45 \cdot 10^{03}$	0.974

that led to destruction of cellulose and hemicellulose structures [29]. Specifically, straw biomass passes through HTC, and cellulose, hemicellulose and their degradation products form the VM of hydrochars. High temperature affects the decomposition of cellulose and hemicellulose. Hemicellulose and cellulose usually decompose completely at treatment temperatures above 230 °C and 270 °C, respectively, which in turn affects the VM content of the hydrochars, resulting in a change in the activation energy [4, 44]. The RS and CS hydrochars at the Stage II reached the minimum E at 200 °C. As the reaction temperature increased further, the $E_{\text{stage II}}$ showed an increasing trend. The results were mainly attributed to oxidative resistance at the beginning of solid products (hydrochars) combustion by hydrothermal treatment. To be more specific, as the increase of reaction temperature, in addition forming fixed carbon with high energy content, is also effective in solid component formation with higher resistance to oxidation [13]. This explains why hydrochars had the highest T_b at 260 °C.

Straw biomass and its hydrochars showed different changes in the A at different reaction temperatures. As indicated in tab. 4, in Stage I, RS, and CS hydrochars showed the highest $A_{\text{stage I}}$ at 200 °C. As the reaction temperature is increased, the $A_{\text{stage I}}$ decreases. The $A_{\text{stage II}}$ of Stage II is much smaller than that of Stage I, and the $A_{\text{stage II}}$ of straw biomass hydrochars in this stage all show a trend of first decreasing and then increasing. The RS hyochar has the lowest $A_{\text{stage II}}$ at 200 °C, and the CS hydrochars is the lowest at 220 °C. The $A_{\text{stage II}}$ indicates the collision frequency associated with promoting the combustion process by increasing the reaction temperature. As the hydrothermal treatment temperature increases, the hydrochar surface area may increase, which may affect the increase in the $A_{\text{stage II}}$ [13].

The analysis of the whole combustion process shows that the HTC significantly affects the dynamic combustion parameters of hydrochars. Therefore, from the point of view of E, the optimal hydrothermal treatment temperature is 260 °C.

Conclusions

The HTC of straw biomass with high ash content was conducted at different reaction temperatures. The conclusions are as foloows.

- Both the RS and CS hydrochar had the highest energetic recovery efficiency at 200 °C, reaching 66.62% and 64.39%, respectively. Overall, during the HTC process of straw biomass, increasing the reaction temperature improved decarboxylation and dehydration processes, decreased H/C and O/C atomic ratios, and raised the FC/VM. At 260 °C, RS and CS hydrochar have similar atomic ratios to lignite while exhibiting the highest heating value, reaching 17.22 MJ/kg and 19.28 MJ/kg, respectively. This has a similar trend to low ash hydrochars. However, the C content of the straw hydrochar was lower than that of the straw raw material at 180 °C, and its ash content increased with the reaction temperature, which is different from the straw biomass with low ash content. High-ash straw biomass can be used to produce high-performance solid fuels.
- The HTC improves the combustion performance of straw biomass. At 180 °C, the SN of hydrochar is the best, which is $5.04 \cdot 10^{-11}$ ($\text{min}^{-2}\text{K}^{-3}$) and $6.42 \cdot 10^{-11}$ [$\text{min}^{-2}\text{K}^{-3}$], respectively, indicating that the solid product combustion performance is the best, which has similar results to the low ash biomass hydrochars.
- Comprehensive consideration of the data of ultimate analysis, proximate analysis, combustion behavior and kinetic analysis, if the hydrochar was used to instead of coal in industrial applications, 260 °C should be recommended as the HTC temperature for high-ash straw RS and CS.

Acknowledgment

The Project is Supported by Inner Mongolia Autonomous Region Natural Science Foundation (2020BS05019), Inner Mongolia University of Science and Technology Innovation Fund (2019QDL-B41) and Key Laboratory of Power Station Energy Transfer Conversion and System of Ministry of Education.

References

[1] Wang, J., *et al*., Combustion Behaviour and Chemical Structure Changes of Enzyme-Treated Coal, *Journal of Thermal Analysis and Calorimetry*, *142* (2020), 3, 1287
[2] Zhang, X., *et al*., Analysis of Yield and Current Comprehensive Utilization of Crop Straws in China, *Journal of China Agricultural University*, *26* (2021), 09, pp. 30-41
[3] Wang, B., *et al*., Distribution Characteristics, Resource Utilization and Popularizing Demonstration of Crop Straw in Southwest China: A Comprehensive Evaluation, *Ecological Indicators*, *93* (2018), Oct., pp. 998-1004
[4] Yao, Z., *et al*., Effects of Hydrothermal Treatment Temperature and Residence Time on Characteristics and Combustion Behaviors of Green Waste, *Applied Thermal Engineering*, *104* (2016), July, pp. 678-686
[5] Cheng, C., *et al*., Hydrothermal Carbonization of Rape Straw: Effect of Reaction Parameters on Hydrochar and Migration of AAEM, *Chemosphere*, *291* (2021), 132785
[6] Volpe, M., *et al*., Hydrothermal Carbonization of Opuntia Ficus-Indica Cladodes: Role of Process Parameters on Hydrochar Properties, *Bioresource Technology*, *247* (2018), Jan., pp. 310-318
[7] Guo, S., *et al*., Characteristic Evolution of Hydrochar from Hydrothermal Carbonization of Corn Stalk, *Journal of Analytical and Applied Pyrolysi*s, *116* (2015), Nov., pp. 1-9
[8] Xu, Z., *et al*., Effect of Inorganic Potassium Compounds on the Hydrothermal Carbonization of Cd-Contaminated Rice Straw for Experimental-Scale Hydrochar, *Biomass and Bioenergy*, *130* (2019), 105357
[9] Cheng, C., *et al*., Hydrothermal Carbonization of Rape Straw: Effect of Reaction Parameters on Hydrochar and Migration of AAEM, *Chemosphere*, *291* (2022), 132785
[10] Ma, Q., *et al*., Effect of Water-Washing of Wheat Straw and Hydrothermal Temperature on Its Hydrochar Evolution and Combustion Properties, *Bioresource Technology*, *269* (2018), Dec., pp. 96-103
[11] Wang, G., *et al*., Hydrothermal Carbonization of Maize Straw for Hydrochar Production and Its Injection for Blast Furnace, *Applied Energy*, *266* (2020), 114818
[12] Yan, W., *et al*., Upgrading Fuel Quality of Moso Bamboo Via Low Temperature Thermochemical Treatments: Dry Torrefaction and Hydrothermal Carbonization, *Fuel*, *196* (2017), May, pp. 473-480
[13] Santos Santana, M., *et al*., Hydrochar Production from Defective Coffee Beans by Hydrothermal Carbonization, *Bioresource Technology*, *300* (2020), 122653
[14] Zang, J., *et al*., A Facile Preparation of Pomegranate-Like Porous Carbon by Carbonization and Activation of Phenolic Resin Prepared Via Hydrothermal Synthesis in KOH Solution for High Performance Supercapacitor Electrodes, *Advanced Powder Technology*, *30* (2019), 12, pp. 2900-2907
[15] Wang, F., *et al*., Mass Transfer Enhancement in Electrode and Battery Performance Optimization of All-Vanadium Flow Based on Channel Section Reconstruction, *Chemical Engineering Journal*, *45* (2023), 138619
[16] Chu, F., *et al*., Analysis of Electrode Configuration Effects on Mass Transfer and Organic Redox Flow Battery Performance, *Industrial and Engineering Chemistry Research*, *61* (2022), 7, pp. 2915-2925
[17] Khoo, C. G., *et al*., Hydrochar Production from High-Ash Low-Lipid Microalgal Biomass Via Hydrothermal Carbonization: Effects of Operational Parameters and Products Characterization, *Environmental Research*, *188* (2020), 109828
[18] Xu, X., *et al.*, The Correlation of Physicochemical Properties and Combustion Performance of Hydrochar with Fixed Carbon Index, *Bioresource Technology*, *294* (2019), 122053
[19] Friedl, A., *et al*., Prediction of Heating Values of Biomass Fuel from Elemental Composition, *Analytica Chimica Acta*, *544* (2005), 1, pp. 191-198
[20] Ping, C, *et al*., Research on the Pyrolysis Kinetics of Blended Coals (in Chinese), *Chinese Society for Electrical Engineering*, *27* (2007), 17, pp. 6-10
[21] Zhang, C., *et al.*, Conversion of Water Hyacinth to Value-Added Fuel Via Hydrothermal Carbonization, *Energy*, *197* (2020), 117193
[22] Liu, J., *et al*., Thermogravimetric Study on Combustion Characteristics of Lignite Semicoke (in Chinese), *Thermal Power Generation*, *42* (2013), 11, pp. 86-92

[23] Shen, D. K., *et al*., Kinetic Study on Thermal Decomposition of Woods in Oxidative Environment, *Fuel*, *88* (2009), 6, pp. 1024-1030
[24] Wang, C., *et al*., Thermogravimetric Studies of the Behavior of Heat Straw with Added Coal during Combustion, *Biomass and Bioenergy*, *33* (2009), 1, pp. 50-56
[25] He, C., *et al*., Conversion of Sewage Sludge to Clean Solid Fuel Using Hydrothermal Carbonization: Hydrochar Fuel Characteristics and Combustion Behavior, *Applied Energy*, *111* (2013), Nov., pp. 257-266
[26] Magdziarz, A., *et al*., Pyrolysis of Hydrochar Derived from Biomass – Experimental Investigation, *Fuel*, *267* (2020), 117246
[27] Wilk, M., *et al*., Hydrothermal co-Carbonization of Sewage Sludge and Fuel Additives: Combustion Performance of Hydrochar, *Renewable Energy*, *178* (2021), Nov., pp. 1046-1056
[28] Nakason, K., *et al*., Hydrothermal Carbonization of Unwanted Biomass Materials: Effect of Process Temperature and Retention Time on Hydrochar and Liquid Fraction, *Journal of the Energy Institute*, *91* (2018), 5, pp. 786-796
[29] Chen, X., *et al*., Conversion of Sweet Potato Waste to Solid Fuel Via Hydrothermal Carbonization, *Bioresource Technology*, *249* (2018), Feb., pp. 900-907
[30] Funke, A., Ziegler, F., Hydrothermal Carbonization of Biomass: A Summary and Discussion of Chemical Mechanisms for Process Engineering, *Biofuels, Bioproducts and Biorefining*, *4* (2010), 2, pp. 160-177
[31] Sabio, E., *et al*., Conversion of Tomato-Peel Waste into Solid Fuel by Hydrothermal Carbonization: Influence of the Processing Variables, *Waste Management*, *47* (2016), Jan., pp. 122-132
[32] Zhang, S., *et al*., Physiochemical Properties and Pyrolysis Behavior Evaluations of Hydrochar from co-Hydrothermal Treatment of Rice Straw and Sewage Sludge, *Biomass and Bioenergy*, *140* (2020), 105664.
[33] Kim, D., *et al*., Upgrading the Fuel Properties of Sludge and Low Rank Coal Mixed Fuel through Hydrothermal Carbonization, *Energy*, *141* (2017), Dec., pp. 598-602
[34] Shrestha, A., *et al*., Study of Hydrochar and Process Water from Hydrothermal Carbonization of Sea Lettuce, *Renewable Energy*, *163* (2021), Jan., pp. 589-598
[35] Zhang, L., *et al*., Hydrothermal Carbonization of Corncob Residues for Hydrochar Production, *Energy and Fuels*, *29* (2015), 2, pp. 872-876
[36] Parshetti, G. K., *et al*., Chemical, Structural and Combustion Characteristics of Carbonaceous Products Obtained by Hydrothermal Carbonization of Palm Empty Fruit Bunches, *Bioresource Technology*, *135* (2013), May, pp. 683-689
[37] Park, S.-W., Jang, C.-H., Characteristics of Carbonized Sludge for co-Combustion in Pulverized Coal Power Plants, *Waste Management*, *31* (2011), 3, pp. 523-529
[38] Liu, H., *et al*., Hydrothermal Carbonization of Natural Microalgae Containing a High Ash Content, *Fuel*, *249* (2019), Aug., pp. 441-448
[39] Jafari, M., *et al*., Preparation and Characterization of Bionanocomposites Based on Benzylated Wheat Straw and Nanoclay, *Journal of Polymers and the Environment*, *26* (2018), 3, pp. 913-925
[40] Wilk, M., *et al*., Upgrading of Green Waste into Carbon-Rich Solid Biofuel by Hydrothermal Carbonization: The Effect of Process Parameters on Hydrochar Derived from Acacia, *Energy*, *202* (2020), 117717
[41] Cai, J., *et al.*, Hydrothermal Carbonization of Tobacco Stalk for Fuel Application, *Bioresource Technology*, *220* (2016), Nov., pp. 305-311
[42] Yao, Z., Ma, X., Characteristics of co-Hydrothermal Carbonization on Polyvinyl Chloride Wastes with Bamboo, *Bioresource Technology*, *247* (2018), Jan., pp. 302-309
[43] Lu, J.-J., Chen, W.-H., Investigation on the Ignition and Burnout Temperatures of Bamboo and Sugarcane Bagasse by Thermogravimetric Analysis, *Applied Energy*, *160* (2015), pp. 49-57
[44] Wu, Q., *et al*., Characterization of Products from Hydrothermal Carbonization of Pine, Bioresource Technology, *244* (2017), Nov., pp. 78-83

Paper submitted: August 13, 2022
Paper revised: October 21, 2022
Paper accepted: October 23, 2022